

## Research Paper

# Evaluation of Cutting Forces and Temperature of Iron-Rich Binder Carbide Tool in Turning of Titanium

Chandrashekar MAHADEVIAH<sup>1)</sup>, Sreenivasa PRASAD<sup>2)</sup>

<sup>1)</sup> *Visvesvaraya Technological University*  
Belagavi, Karnataka state, India  
e-mail: nie.chandrashekar@gmail.com

<sup>2)</sup> *Jagadguru Sri Shivarathreeswara University, SJCE*  
Mysuru-570006, Karnataka state, India

The machining of titanium has been understood to be challenging and costly due to its material properties such as low thermal conductivity, low modulus of elasticity, high strength at elevated temperatures and chemical reactivity. This work aims to study the effect of iron as a partial substitution along with cobalt binder as the tool material for machining of titanium alloy. In this work, iron-rich binder tool (WC-Co-Fe) and cobalt binder tool (WC-Co) samples were produced by powder metallurgy route using powders with a mean particle size of less than 0.5  $\mu\text{m}$ . Next, the evaluation of mechanical properties and phase analysis were performed. Turning experiments were conducted at various cutting speeds, feed and depth of cut (DOC), to evaluate the effects of iron-rich binder on flank wear, cutting forces and cutting temperature. The obtained results of turning experiments reveal that iron-rich binder tends to increase cutting performance in comparison to conventional WC-Co composite cutting tools.

**Key words:** titanium; cutting tools; tungsten carbide; cobalt; iron.

## 1. INTRODUCTION

Despite the fact that titanium is considered as difficult to cut material, its usage has been increasing gradually in engineering sectors such as marine, aerospace, biomedical, automotive and petrochemical industries, where prime requirement is a high strength at elevated temperature, and resistance to wear and chemical degradation. Currently, many studies are conducted in view of increasing tool performance at high cutting speed to improve productivity. Titanium alloys are broadly classified into three main categories, based on stabilizers such as alpha alloys, alpha-beta alloys and beta alloys, all these alloys have different

properties and can be used accordingly. Ti-6Al-4V is widely used in aerospace and medical engineering. It is an alpha-beta alloy that is heat treatable to achieve an increase in strength [1, 2].

One drawback of these alloys is their poor machinability. Despite their several advantages, titanium and its alloys pose several challenges for machining due to properties such as high strength which converts to low cutting speeds, low modulus of elasticity and poor thermal conductivity. Longitudinal turning is a continuous machining operation. The material removal rate ( $Q$ ) is a good measure of how fast the machining operation removes the material from the workpiece. The material removal rate is calculated with Eq. (1.1)

$$(1.1) \quad Q = V_c F_n A_p K_r,$$

where  $V_c$ ,  $F_n$ ,  $A_p$ , and  $K_r$  represent the cutting speed [m/min], feed rate [mm/rev], depth of cut [mm] and entering angle [°], respectively [3, 4].

At critical cutting speed, localized shear involved in the segmented chip formation leads to the generation of cyclic forces which results in the rough machined surface, the chatter and chipping of cutting edge [5]. Machining of titanium alloys is a typical case of distinct gross inhomogeneous plastic deformation involving periodic upsetting and intense shear localization in a narrow band. It is suggested that intense contact of the chip at or near the tip of the tool for a substantial time leads to a reaction between tool and chip causing high tool wear [6].

The low machinability of titanium alloys due to the low thermal conductivity and high microhardness of these materials leads to severe and premature tool wear in the dry machining process. Thermal and mechanical analysis revealed two important phenomena. First, the thermal softening which results in a lowering of the yield stress when the temperature increases, and secondly the strain-rate hardening which increases the hardness of the material. Increasing the hardness in machining implies a systematic increase in the level of cutting force. Indeed, an increase in the cutting speed raises the temperature at the tool-workpiece interface and increases at the same time the strain rate. Both phenomena occur simultaneously and reflect two opposite effects. It was concluded from different analyses that the Ti-6Al-4V alloy is more sensitive to thermal softening [7].

FRIEDRICH and KULKARMI [8] concluded that the springback in the milling operation is a linear function of tool edge radius and the ratio of material hardness to elastic modulus. It can be calculated using the following equation:

$$(1.2) \quad S = kr(H/E),$$

where  $S$  is the springback,  $k$  is constant,  $r$  is the cutting edge radius,  $H$  and  $E$  are the hardness and Young's modulus of the workpiece material, respectively.

Significantly, low Young's modulus and reasonably high hardness make titanium alloy highly elastic which cause excessive workpiece deflection and small plastic deformation. Thus, there is a bouncing action as the cutting edge comes in contact with the workpiece during machining processes under cutting pressure. The workpiece tends to move away from the cutting tool unless deep cuts are performed, or rigid backup is applied. This tendency also leads to a less effective clearance angle at the flank face, enhanced friction, and chatter.

MASAFUMI [9] and MOZAMMEL *et al.* [10] investigation shows that the cutting temperature became higher when there was an increase in cutting speed, feed or depth of cut. Increase in cutting speed and feed was more influential on the value than the increase in the depth of cut when two cutting conditions with the same material removal rates were compared. The main reasons for this are lower thermal conductivity and higher cutting forces.

Carbide tools are the preferred tools for machining titanium and its alloys. Cobalt is the most preferred binding material because it forms a solid solution with tungsten carbide, which results in a hard phase in microstructure and good mechanical properties. Addition of refractory elements such as iron or nickel along with cobalt improves the performance of the WC-based cemented carbides. In this regards, iron has the highest affinity for carbon compared to nickel so it can form a metal-to-carbon bond relationship. Moreover, iron has good wettability and solubility for WC lowering the ternary eutectic temperature compared to cobalt [11–13].

In view of the above literature survey, it is concluded that to overcome concern related to the machining of titanium economically, a number of researches are in progress to improve cutting tool material. The aim of the study is to enhance the performance of cutting tool material by adding iron as a partial substitution to straight carbides (WC/Co), which is motivated by economic consideration.

## 2. MATERIALS AND METHODS

### 2.1. Preparation of test samples

The workpiece used in this study was a Ti6Al4V bar with a diameter of 50 mm. The chemical composition of the workpiece is presented in Table 1. In

**Table 1.** Chemical composition of titanium alloy (Ti-6Al-4V).

| Elements | V%   | Fe%  | Ti%   | Al%     |
|----------|------|------|-------|---------|
|          | 3.82 | 0.15 | 91.15 | Balance |

the present investigation, tungsten carbide, cobalt and iron powders of average particle size less than 0.5  $\mu\text{m}$  were used to prepare the sample through/using powder metallurgy route [14].

The test samples were produced through powder metallurgy route at Central Manufacturing Technology Institute, Bangalore, Karnataka. Two different samples were manufactured. As per literature survey [15], it is recommended to use 5 to 12% binder in composition, for the initial study, with 0.5% of iron added randomly as a partial substitution along with cobalt for sample B. Further, increasing percentage will be the future scope of the study. The test samples' compositions are shown in Table 2.

**Table 2.** Samples' composition (% by volume).

|                       | Sample A | Sample B |
|-----------------------|----------|----------|
| Tungsten Carbide (WC) | 95       | 95.0     |
| Cobalt (Co)           | 5        | 4.5      |
| Iron (Fe)             | 0        | 0.5      |

The first stage of production is blending of raw materials with additives and lubricants by using a ball mill at 60% of the critical rotational speed for 10 hours. After blending it uniformly, the blended mixture was pressed using a universal testing machine (UTM) to a size of  $12 \times 6$  mm under pressure of 200 MPa. After pressing, the samples were sintered at a temperature of 1350°C for one hour in a furnace with a continuous flow of hydrogen. As a secondary operation, samples were brazed to a standard tool shank. Tool geometry was generated as per standard.

## *2.2. Evaluation of micro-structures and mechanical properties*

After sintering, mechanical properties such as hardness and toughness were investigated for each sample. The hardness (HV) of sample B with cobalt (Co) and iron (Fe) was higher than that of sample A with only cobalt (Co) binder phase for the same tungsten carbide concentration, and vice versa for fracture toughness [ $\text{MPa}\cdot\text{m}^{1/2}$ ] which is derived by performing the Palmquist indentation method. Also, it indicates the presence of harder binder phase in sample B. Figure 1 shows related hardness and toughness values for each sample.

The scanning electron micrographs are shown in Fig. 2 (sample A and B). The microstructure image shows the presence of carbide and binder phases. These phases are critical for the mechanical properties of the cutting tool. It consists of tungsten carbide in a binder phase, characterized by dark-black cores with the light grey rim. During the sintering process, tungsten carbide crystals develop

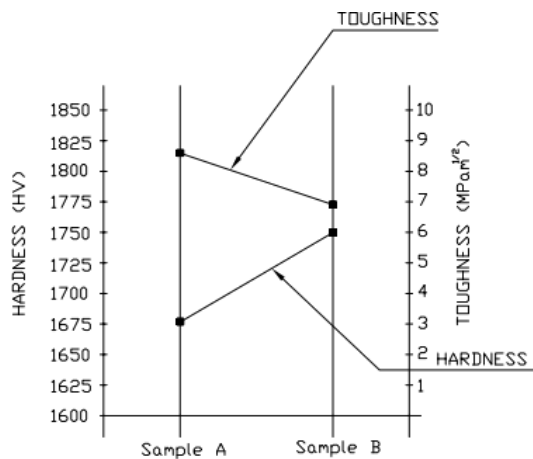
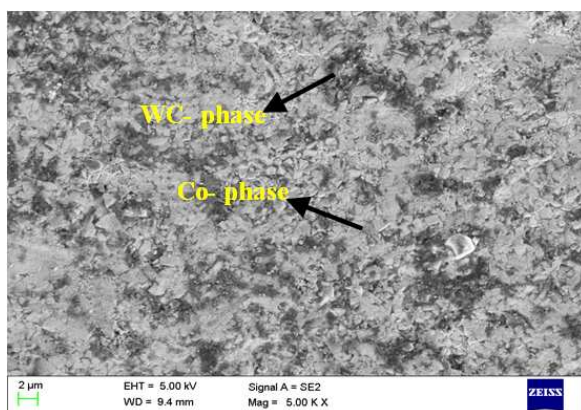


FIG. 1. Hardness/toughness in sample A and sample B.

a)



b)

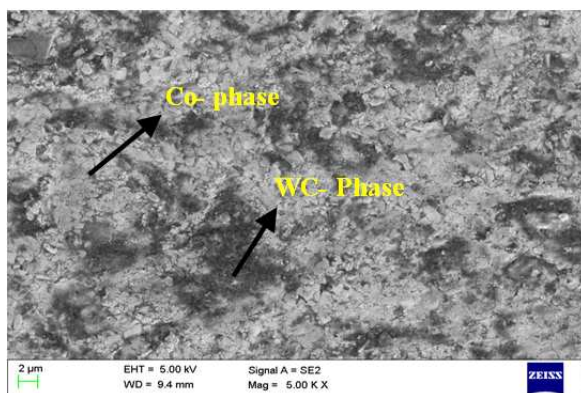


FIG. 2. SEM images of sample A (a) and sample B (b).

well-defined crystallographic facets. It is significant that the grain growth of WC in cemented carbides generally occurs in two modes, namely coalescence and solution-precipitation process. Figure 2 (sample B) shows a good particle fusion in the microstructure. Therefore, the mechanical properties are better as compared to sample A.

XRD analysis was carried out to study the crystal structure. Figure 3 shows that sample A is a W-C-Co alloy, which exists in the allotropic form of hexagonally close-packed (HCP) phase. Whereas in specimen B it is found that the binder phase is composed of both body-centered cubic and hexagonally close packed phases, in which the inclusion of cobalt into iron takes place to form the cobalt-iron phase (Co-Fe).

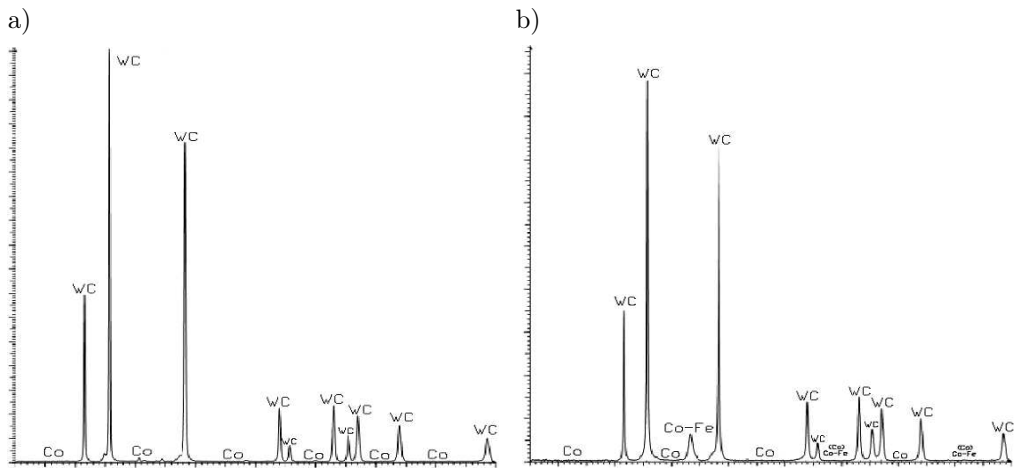


FIG. 3. X-ray spectra: a) of a WC-Co composite with 5 Wt% Co (sample A), b) of a WC-Co-Fe composite with 4.5 Wt% Co and 0.5 Wt% Fe (sample B).

### 3. EXPERIMENTAL PROCEDURE

Machinability is a way to measure and classify how easily a particular work-piece material can be machined by a cutting tool in a manner such that certain predetermined levels of form, size and degree of roundness of the surface can be achieved. To measure cutting forces, namely thrust force ( $f_x$ ), feed force ( $f_y$ ) and tangential force ( $f_z$ ), the lathe tool post was fitted with a dynamometer, and force values were recorded through digital instrument which was interfaced with dynamometer, under the following conditions: cutting speeds 10, 20, 30, 40, 50, 60 m/min, feed = 0.25 mm/rev, depth of cut = 0.5 mm, KALIDAS [16], cutting time was 30 seconds for each experiment. Cutting temperatures were measured using a non- contact infrared thermometer at different feed rates, keeping cut-

ting speed (30 m/min) and depth of cut 0.5 mm constant. No coolants or cutting fluids were used to facilitate collecting required data.

The wear resistance property of the samples was evaluated in actual turning experiments under the following conditions: cutting speeds 30 m/min and 60 m/min, keeping feed = 0.25 mm/rev and depth of cut = 1 mm, constant at both cutting speed with coolant at a flow rate of 30 l/min and at a pressure of 12 kg/m<sup>2</sup> [17]. The flank wear was measured at regular intervals of 30 seconds [18].

#### 4. RESULTS AND DISCUSSION

##### *4.1. Effect of cutting speed and depth of cut on cutting forces*

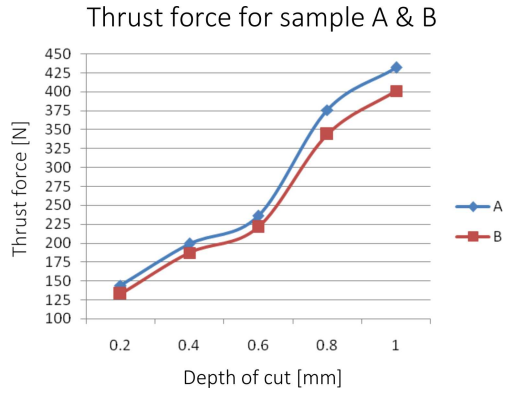
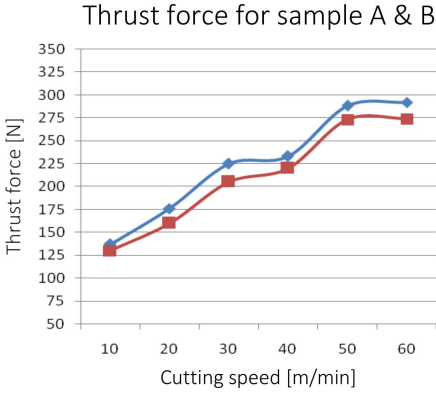
Cutting force is an important parameter in a cutting process, which has a great influence on cutting temperature, tool life, machining precision, etc. The cutting forces are induced by the action of the cutting tool to the workpiece, and the rate of change of cutting forces is measured with a dynamometer. The main reason for conducting this experiment was to investigate how the addition of iron to cobalt binder content affects the cutting tool performance while turning titanium alloy (Ti-6Al-4V). There are two samples that are important to compare in order to see the influence of iron content. For both samples the effect of cutting speed on the cutting force is shown in Figs. 4a–c in graph data it is observed that the all three cutting force components increase linearly with cutting speed. They increase initially with cutting speed up to 30 m/min due to work-piece strain hardening and remain constant from 30 to 45 m/min, which can be attributed to thermal softening due to increased cutting temperature. A sudden increase in the forces was observed beyond cutting speed of 45 m/min. Also, it is observed from the plotted graph that cutting force and feed force increase almost linearly with the increase in depth of cut. Even though the increase in cutting force was identical in both samples A and B from beginning to end for a set cutting time, cutting force in sample B is smaller than in sample A.

Among the force components, cutting force and feed force prominently influence power consumption and the most common equation available for the estimation of cutting force ( $F_c$ ) is given by Eq. (4.1):

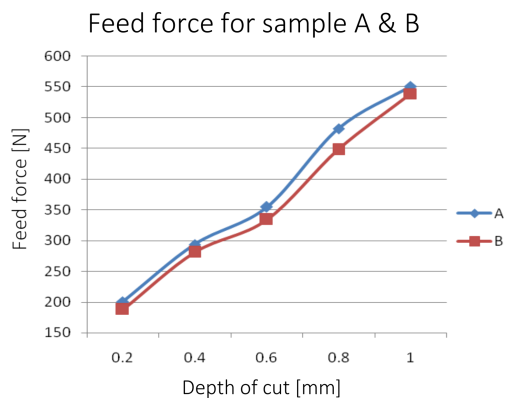
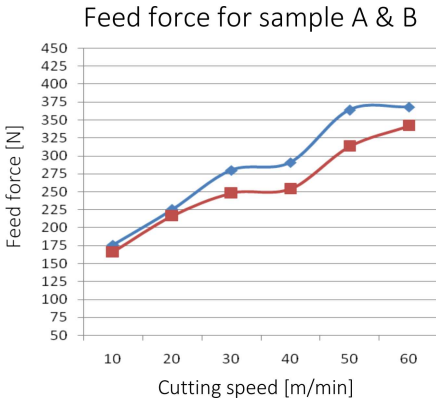
$$(4.1) \quad F_c = k_c \cdot \text{DOC} \cdot F_n,$$

where DOC is depth of cut [mm],  $F_n$  is feed [mm/rev] and  $k_c$  is the specific cutting energy coefficient [N/mm<sup>2</sup>]. According to Eq. (1.1), cutting force is influenced by the depth of cut, feed, and specific cutting energy coefficient [19].

a)



b)



c)

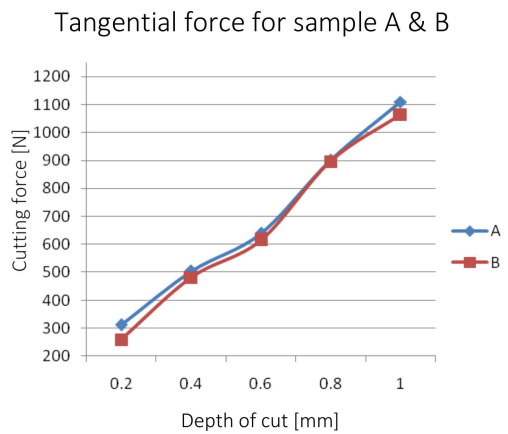
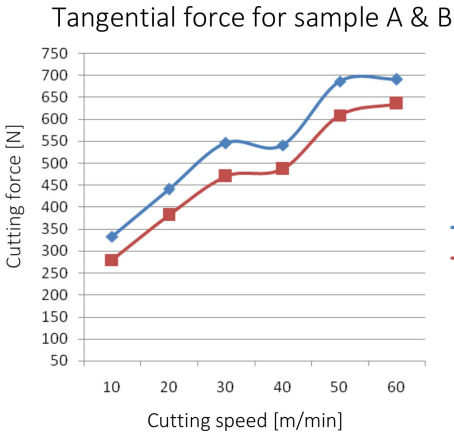


FIG. 4. Effect of cutting speed and depth of cut on the cutting forces for sample A and sample B: a) variation of thrust force of sample A and B at different cutting speeds and depth of cut, b) variation of feed force of sample A and B at different cutting speeds and depth of cut, c) variation of cutting force of sample A and B at different cutting speeds and depth of cut.

#### 4.2. Tool wear measurement

Flank wear is a major form of tool wear in metal cutting, in which the portion of the tool in contact with the finished part erodes. The rate of flank wear measured with a toolmakers microscope is presented in Figs. 4–7. The main reason to conduct this experiment was to investigate how the addition of iron to cobalt binder content affects the cutting tool wear while turning titanium alloy (Ti-6Al-4V).

In Fig. 5a, at cutting speed of 30 m/min, even though wear behaviour was identical in both samples A and B from beginning to end for a set cutting time, sample A showed more wear at the beginning compared to sample B, that is, for sample A measured flank wear value was 0.21 mm, whereas for sample B it was 0.13 mm at 30 m/min cutting speed. In Fig. 5b, it can be observed that at cutting speed of 60 m/min, sample B showed very small flank wear. In addition, at the end of set cutting time wear remained constant when compared to sample A. The plotted graph shows that the new material with iron content under investigation displays a distinct improvement in life at higher cutting speeds than the one without iron at higher cutting speeds.

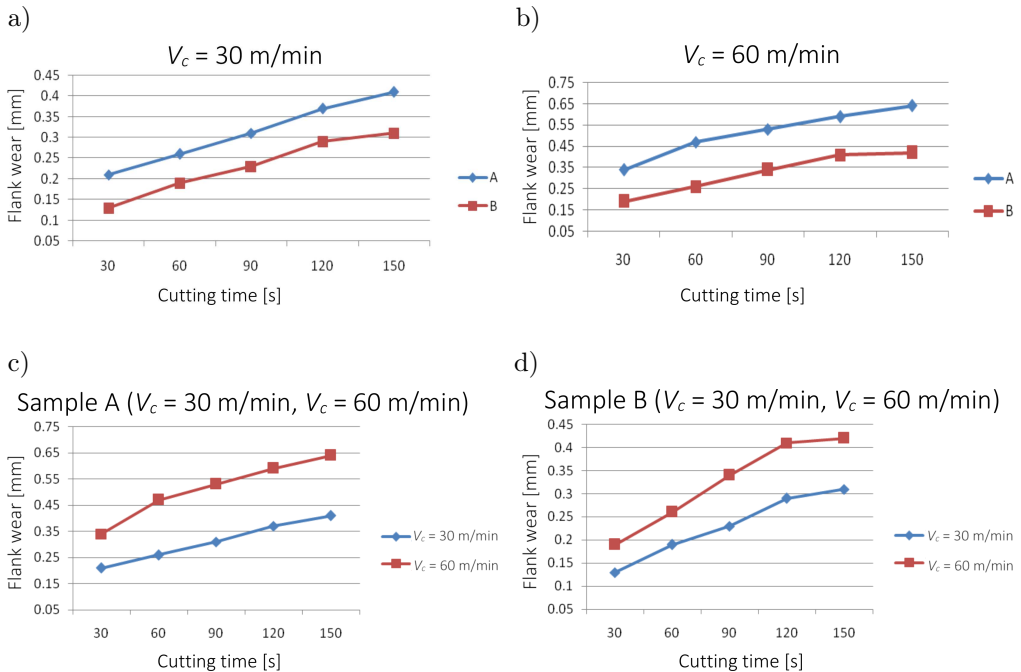


FIG. 5. Typical wear rate of sample A and sample B at cutting speeds: a) wear tests of sample A and B at  $V_c = 30$  m/min, b) wear tests of sample A and B at  $V_c = 60$  m/min, c) wear tests of sample A at  $V_c = 30$  and 60 m/min, d) wear tests of sample B at  $V_c = 30$  and 60 m/min.

It is evident from the SEM images of cutting edges of both samples that cutting edges in sample A were chipped off at a cutting speed of 60 m/min, whereas for sample B it was smooth wear. Also, it is observed in all graphs that wear on sample B was so small that it could not have a significant effect on the tool during machining, in sample B flank wear rate reached a steady state following rapid initial wear under the same cutting condition.

Figure 6 shows typical wear pattern of samples as seen in SEM micrographs, after turning at a cutting speed of 60 m/min. By visual examination, on sample A, local flank wear so-called notch wear on the main and minor cutting edges along with non-uniform abrasive wear were noticed. Notching is mainly caused by a fracture process, and it happens when excessive localized damage occurs at the flank and rake face simultaneously. The notch will cause poor surface finish; further, it leads to fracture wear. Whereas, for sample B wear was smooth, which did not lead to any catastrophic tool failure. Iron has good wettability and solubility for tungsten carbide. The addition of iron enhances the fusion of tungsten carbide particles, which increases the overall strength of sample as compared to the sample without iron.

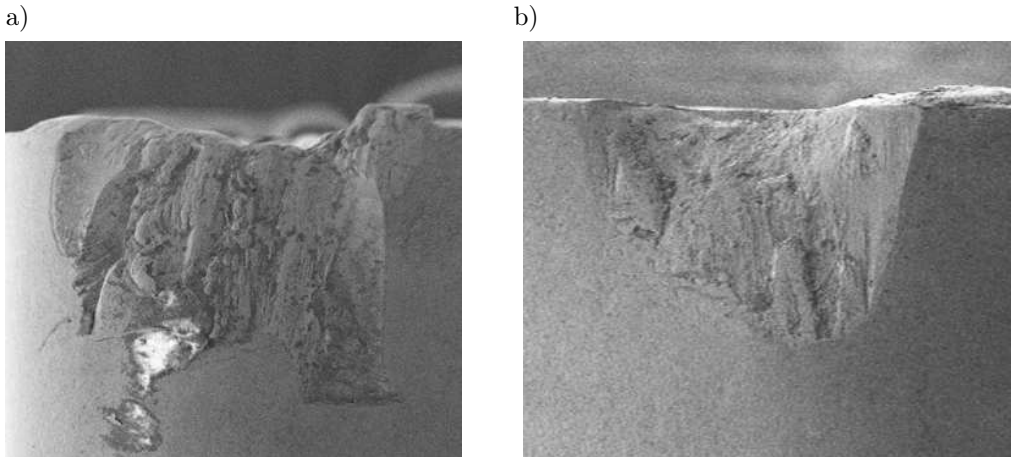


FIG. 6. Typical cutting edge wear of sample A (a) and sample B (b) at a cutting speed of 60 m/min.

#### *4.3. Measurement of cutting temperature rate*

The cutting temperature generated during the machining of titanium alloys plays an important role in the subsequent surface integrity of the machined workpiece. Cutting temperature is the function of cutting speed and feed rate. The excessive heating can lead to a reduction in tool life.

The average cutting speed can be specified using the following equation:

$$(4.2) \quad \Theta_t = V^{0.5} f^{0.3},$$

where  $\Theta_t$  is the average cutting temperature,  $V$  is the cutting speed, and  $f$  is the feed rate [18].

Figure 7 shows the effect of feed and cutting speed on the tool temperature for both sample A and sample B. A linear increase in temperature is recorded for the increase in feed rate and cutting speed, keeping the depth of cut = 0.5 mm constant. In correlation to Eq. (4.2), it was observed that when cutting speed is increased, the contact between the tool and chip increases, which in turn increases the amount of heat generated in the cutting zone. Titanium material and low thermal conductivity property further lead to increased cutting temperature during the machining. Also, it is observed that increasing the feed rate along with cutting speed generates more friction between the workpiece and tool, which further rises cutting temperature.

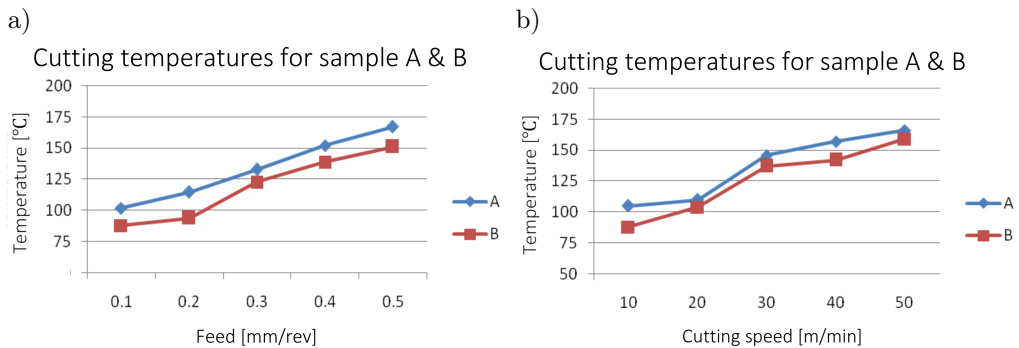


FIG. 7. Influence of feed and cutting speed on cutting temperatures of sample A (a) and sample B (b).

The plotted graph clearly shows that the rate of heat transfer for sample B, which contains iron as a partial substitution along with cobalt binder, is higher compared to sample A (WC-Co).

#### 4.4. Tool life

Based on the data from tool wear measurement of both sample A and sample B at 30 m/min cutting speed, it is observed that it takes 90 s for sample A to reach flank wear of 0.3 mm, while it takes 120 s for sample B to show the same wear rate. Also, the plotted graphs of both cutting forces against cutting speed, depth of cut and cutting temperature against feed and cutting speed reveal that sample B can withstand more load compared to sample A.

## 5. CONCLUSIONS

This research focused on the evaluation of cutting forces, cutting temperature and flank wear of the iron-rich binder carbide cutting tools in turning of titanium alloys. Newly developed samples were subjected to various tests in comparison to straight carbides (WC/Co). Following are the findings obtained from test results.

- 1) The characterization study reveals that iron-rich binder carbide cutting tool material shows good mechanical properties.
- 2) Measured cutting force values confirm that the cutting force over iron-rich binder tool is lower compared to cobalt binder tool for the same cutting speed.
- 3) Plotted graph of cutting temperature at different cutting feeds and speeds reveals that the rate of heat transfer in iron-rich binder tool is higher compared to cobalt binder tool.
- 4) Plotted wear rate graphs at different cutting speeds reveal that iron-rich binder tool shows improved tool life compared to cobalt binder tool.

## 6. FUTURE RESEARCH STUDY

Additional experimentation is planned to correlate the anisotropy of dimensional changes to the material and the geometry of the tool samples in turning of titanium. The anisotropy can be responsible for the changes in the dynamic behavior of the cutting process, that is, when the tool cutting edge passes from a crystal grain to another, and different mechanical properties starting from the grain boundary are found. These physical variations are considered to be responsible for the micro-vibrations of the tooltip both in the crossfeed and infeed directions. Hence, the influences of microstructural anisotropy on the mechanical response of the tool material will be discussed.

## REFERENCES

1. EZUGWU E.O, WANG Z.M., *Titanium alloys and their machinability – a review*, Journal of Materials Processing Technology, **68**(3): 262–274, 1997.
2. PAULO DAVIM J. (ed.), *Machining of Titanium Alloys*, Materials Forming, Machining and Tribology, Springer, Berlin/Heidelberg, 2014, doi: 10.1007/978-3-662-43902-9\_1, 2014.
3. AHSAN K.B., MAZID A.M., CLEGG R.E., PANG G.K.H., *Study on carbide cutting tool life using various cutting speeds for  $\alpha$ - $\beta$  Ti alloy machining*, Journal of Achievements in Materials and Manufacturing Engineering, **55**(2): 601–606, 2012.

4. EZUGWU E.O., WANG Z.M., MACHADO A.R., *Wear of coated carbide tools when machining nickel (Inconel-718) and titanium base (Ti-6Al-4V) alloys*, Tribology Transactions, **43**: 263–268, 2000.
5. SUN S., BRANDTM., DARGUSCH M.S., *Characteristics of cutting forces and chip formation in machining of titanium alloys*, International Journal Machine Tools and Manufacturing, **49**(7–8): 561–568, 2009.
6. KOMANDURI R., *Some clarifications on the mechanics of chip formation when machining titanium alloys*, Wear, **76**: 15–34, 1982.
7. NOUARI M., MAKICH H., *Experimental investigation on the effect of the material microstructure on tool wear when machining hard titanium alloys: Ti-6Al-4V and Ti-555*, International Journal of Refractory Metals and Hard Materials, **41**: 259–269, 2013.
8. FRIEDRICH C.R., KULKARMI V.P., *Effect of workpiece springback on micro-milling forces*, Microsystem Technologies, **10**: 472–477, 2004
9. KIKUCHI M., *The use of cutting temperature to evaluate the machinability of titanium alloys*, Acta Biomaterialia, **5**(2): 770–775, 2009, doi:10.1016/j.actbio.2008.08.016.
10. MIA M., KHAN A., DHAR N.R., *High-pressure coolant on flank and rake surfaces of tool in turning of Ti-6Al-4V: investigations on surface roughness and tool wear*, International Journal of Advance Manufacturing Technology, **90**(5–8): 1825–1834, 2017, doi: 10.1007/s00170-016-9512-5.
11. GILLE G., SZESNY B., DREYER K., VAN DEN BERG H., SCHMIDT J., GESTRICH T., LEITNER G., *Submicron and ultrafine grained hard metals for microdrills and metal cutting inserts*, International Journal of Refractory Metals and Hard Materials, **20**(1): 3–22, 2002, doi: 10.1016/S0263-4368(01)00066-X.
12. FANG Z.Z., WANG X., RYU T., HWANG K.S., SOHN H.Y., *Synthesis, sintering, and mechanical properties of nanocrystalline cemented tungsten carbide – a review*, International Journal of Refractory Metals and Hard Materials, **27**(2): 288–299, 2009, doi: 10.1016/j.ijrmhm.2008.07.011.
13. DE MACEDO H.R., DA SILVA A.G.P., DE MELO D.M.A., *The spreading of cobalt, nickel and iron on tungsten carbide and the first stage of hard metal cutting*, Material Letters, **57**(24–25): 3924–3932, 2003, doi: 10.1016/S0167-577X(03)00242-8.
14. DAVIS J.R., *ASM specialty handbook: tool materials. General guidelines for selecting cutting tool materials*, ASM International, 1995, www.asminternational.org.
15. KALIDASS S., RAVIKUMAR T.M., *Cutting force prediction in end milling process of AISI 304 steel using solid carbide tools*, International Journal of Engineering Transactions A: Basics, **28**(7): 1074–1081, 2015.
16. RAMANA M.V., RAO G.K.M., RAO D.H., *Experimental investigations on tool wear in turning of Ti-6Al-4V alloy under different machining environmental conditions*, International Journal of Manufacturing Research, **11**(4): 339–355, 2016, doi: 10.1504/IJMR.2016.10003302.
17. GHANI J., CHE HARON C., KASIM M., SULAIMAN M., TOMADI S., *Wear mechanism of coated and uncoated carbide cutting tool in machining process*, Journal of Materials Research, **31**(13): 1873–1879, 2016, doi: 10.1557/jmr.2015.382.

18. SAHU D.K., SEN P.K., SAHU G., SHARMA R., BOHIDAR S., *A review on effect of cutting parameters on cutting force in turning process*, Engineering Science and Technology: An International Journal, **5**(5): 332–337, 2015.
19. LOWEN E.G., SHAW M.C., *On the analysis of cutting tool temperatures*, Transactions of ASME, **76**: 217–231, 1954.

*Received February 11, 2018; accepted version June 13, 2018.*

---